Astron. Astrophys. 315, L93–L96 (1996)

ASTRONOMY AND ASTROPHYSICS

ISOCAM observations of the Antennae Galaxies⋆

L. Vigroux[1], F. Mirabel[1], B. Altiéri[3], F. Boulanger[2], C. Cesarsky[1], D. Cesarsky[2], A. Claret[1], C. Fransson[3], P. Gallais[1], D. Levine[3], S. Madden[1], K. Okumura[3], and D. Tran[1]

[1] CEA/DSM/DAPNIA Service d'Astrophysique, F-91191 Gif-sur-Yvette, France

[2] Institut d'Astrophysique Spatiale, F-91405 Orsay, France

[3] ISO Science Operation center,Astrophysics Division of ESA, Villafranca del Castillo, P.O. Box 50727, E-28080 Madrid, Espagne

Received 16 July 1996 / Accepted 29 August 1996

Abstract. We have mapped the Antennae Galaxies (NGC 4038/39) in the 6.7 and 15 μm continuum emission using ISOCAM[1] with $\simeq 5-8$" resolution. Spectrophotometric observations with the CVF in the spectral range 5.5 to 16.5 μm have also been obtained. We compare the distribution of the infrared emission in the 2 nuclei and in the overlap region where the disks of the galaxies collide. The emission longward of 12.5 μm is dominated by ionized gas and by reprocessing of UV flux by dust. The overlap region is the most active star forming area in the system and contributes to more than half of the total infrared luminosity between 12.5 and 18 μm. The brightest knot in the overlap region has a surface brightness at 15μm which is 5 times larger than the nuclei of the parent galaxies. From the [Ne III] and [Ne II] lines, we estimate a lower limit to the effective temperature of the ionizing stars of 39,500 K and 37,000 K in the overlap region and the nuclei, respectively.

Key words: galaxies: individual: NGC 4038/39 – galaxies: individual: Antennae Galaxies – infrared: interstellar: continuum – stars: formation

1. Introduction

As a result of the IRAS survey, it has become evident that for bolometric luminosities $\geq 10^{11}$ $L_\odot$, infrared-luminous galaxies are the dominant population of objects in the local universe (Soifer *et al.* 1986). There is strong evidence that such intense infrared radiation can be a consequence of bursts of star formation triggered by collisions and mergers between gas-rich spiral galaxies (Sanders *et al.* 1988). The bulk of the infrared emission originates from dust heated by intense starbursts in giant molecular clouds.

The unprecedented capabilities of ISOCAM during the Performance Verification (PV) phase (Césarsky et al. 1996) were used to map NGC 4038/39 (Arp 244 = VV 245 = 'The Antennae'), the prototype nearby early merger system. The Antennae appear to be two overlapping, late-type spiral disk galaxies with the nuclei separated by $\sim$ 15 kpc. At a distance of 20 Mpc the total infrared luminosity measured by IRAS is 10^{11} $L_\odot$. CO interferometer observations (Stanford *et al.* 1990) show that $\sim$ 60% of the $3.9\,10^9$ $M_\odot$ of molecular gas in the system (Sanders & Mirabel 1985) is concentrated in the two nuclei and in an extended off-nuclear complex where the two disks overlap.

2. Observations and Data Analysis

The Antennae Galaxies have been used as template galaxies to test the ISOCAM observing modes during the ISO[2] PV Phase. They were observed in most of the observing modes of ISOCAM using various parameters. The results presented in this paper are based on two set of observations : large raster maps with the 2 filters LW2 (5 - 8 μm) and LW3 (12 - 17 μm) and the 3 $''$ pixel field of view lens. The raster consisted of 10×6 positions with steps of 48 $''$. Integration time was 5 s. A full CVF scan was made from 5.5 μm to 16.5 μm using the smallest possible increment, 0.1 μm step and the 6 $''$ pixel field of view. At each CVF step, 12 images of 2 s integration time were made.

The data analysis was performed using the CAM Interactive Analysis (CIA)[3]. For the raster map, we subtracted a dark frame which was extracted from the calibration data base. The image was corrected using a flat field calculated from the images themselves using a median filtering technique on void regions of the map. Deglitching of cosmic ray induced spikes was performed using the multi resolution deglitching algorithm (Starck

Send offprint requests to: L. Vigroux

⋆ Based on observations with ISO, an ESA project with instruments funded by ESA Member States (especially the PI countries: France, Germany, the Netherlands and the United Kingdom) and with participation of ISAS and NASA.

[1] see Cesarsky *et al.*, 1996

[2] see Kessler *et al.*, 1996

[3] CIA is a joint development by the ESA astrophysics division and the ISOCAM consortium led by the ISOCAM PI, C. Césarsky, Direction des Sciences de la Matière, C.E.A., France

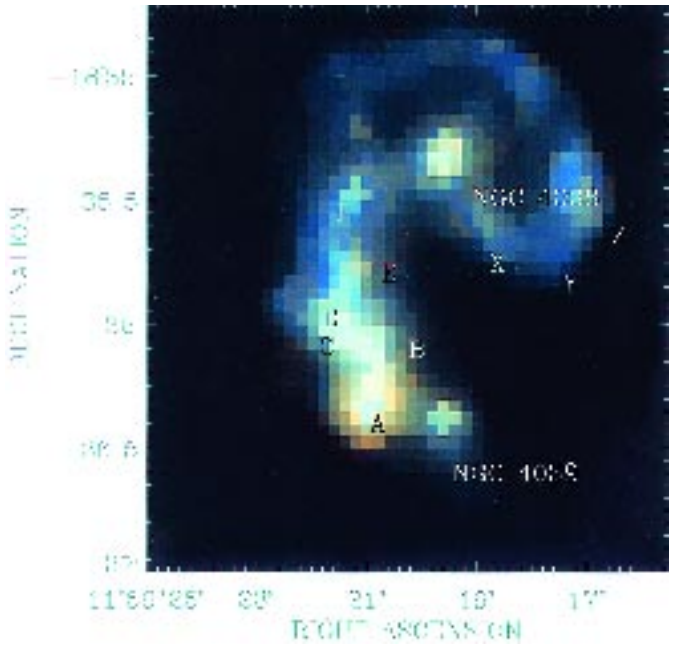

Fig. 1. Color-composite of the LW2 and LW3 maps of the Antennae Galaxies. Blue indicates a high LW3 to LW2 ratio; red a low ratio.

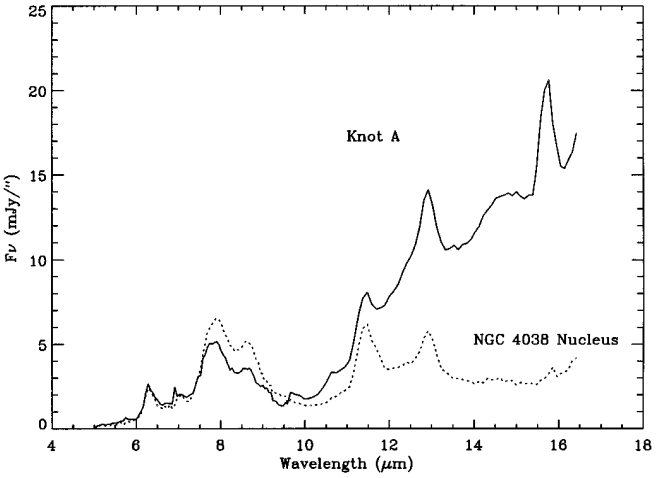

Fig. 2. The CVF spectrum of knot A in the overlap region and the NGC 4038 Nucleus.

et al. 1996). Corrections for transient and memory effect (see Cesarsky et al., 1996) were done with an exponential transient fitting method (Starck et al. 1996). For the CVF, we used library dark and flat field frames. Deglitching was performed using a modified kσ-clipping method which analyzes the tracks of the glitches in the images. A few robust glitches, located on large spectral or spatial gradients of the data were removed by hand. The stray light pattern known to be present with the CVF and 6 $''$ lens combination was removed by using the average pattern observed during CVF scans of the zodiacal background. We used the standard calibration data base for the wavelength and photometric calibrations.

3. Broad Band Imaging

The 2 images obtained with the LW2 and LW3 filters have been combined to create a color image (figure 1). The color code from blue to red corresponds to an increase of the LW3 to LW2 ratio. From the CVF spectrum of the Antennae (figure 2), we see that the LW2 band is dominated by PAH-like emission features, while thermal emission from hot dust and ionized neon lines are the main features in the LW3 band. The ISOCAM image reveals the main star forming regions and the diffuse interstellar emission. The emission is very clumpy and bright knots dominate the infrared emission. Most of these knots have been observed in Hα, CO, (Keel *et al.* 1986; Stanford *et al.* 1990) and radio continuum (Hummel and Van der Hulst 1986). The most conspicuous knots and the nuclei of the two galaxies have been labeled in figure 1. Knots A, B, C, D, and E are in the region where the disks of the 2 galaxies overlap and correspond to clumps seen in the CO aperature synthesis of Stanford *et al.* (1990), and discrete radio knots (Hummel and van der Hulst (1986). Knots X,Y, and Z correspond to the ring of HII regions west of the NGC 4038 nucleus. New photometric fluxes from ISOCAM are given in table 1 along with 6 cm, Hα and CO($1 \rightarrow 0$) data (Stanford *et al.* 1990; Keel *et al.* 1989). The photometry of knot A is in good agreement with the 10 μm observations of Wright *et al.* 1988 (45 ± 12 mJy in a $5''$ aperture at 10 μm).

The brightest spot in the infrared does not coincide with either of the two nuclei, but with the overlap region. Knot A alone, contributes 18% of the total luminosity at 15 μm. It is almost 100 times brighter in the LW3 band than the nucleus of NGC 4039 (see table 1). The overlap region as a whole contributes roughly half of the total luminosity. Similarly, the emission at 6 cm is dominated by the overlap region rather than the bulk of the galaxies. The CO ($1 \rightarrow 0$) emission in the individual knots of the overlap region is roughly proportional to the LW3 emission, while the 2 nuclei are relatively much brighter in CO, than in LW3. In CO, the brightest single spot is the nucleus of NGC 4038, and even the nucleus of NGC 4039 is brighter than any of the individual clumps in the overlap region except knot A. In contrast to M51 (Sauvage *et al.* 1996), there is no correlation between the LW3 luminosity and the Hα luminosity. This absence of correlation is likely due to the high extinction found in the overlap regions. An average extinction of A_v=30 has been derived from the ISO SWS spectra in the overlap region (Kunze *et al.* 1996). In these regions of large extinction, the 15 μm emission should be a much better tracer of star formation than Hα (see also Sauvage *et al.*, 1996). The overlap region is the most active star forming area of the system.

4. CVF spectra

The spectrum of knot A in the overlap region and the nucleus of NGC 4038 is shown in figure 2. The knot A spectrum is characteristic of an active starburst and is dominated by PAH-like emission bands at 6.2, 7.7 8.4 and 11.3 μm and the [Ne II] line at 12.8 μm. As seen in diffuse interstellar medium, a high

Table 1. Flux values for the LW2 and LW3 filters along with CO($1 \rightarrow 0$), 6 cm and Hα data (Hummel and van der Hulst 1989); Keel *et al.* 1989; Stanford *et al.* 1990).

knots	LW3/LW2	LW3 (mJy)	LW2 (mJy)	F_{CO} (Jy km s^{-1})	S6cm (mJy)	H_α
N4039	1.0	0.5	0.5	46.0	4.0	5.1
N4038	1.8	12.1	6.8	159.0	6.0	6.5
A	2.6	49.7	19.1	141.0	16.0	11.3
B	1.0	10.1	9.8	29.0	9.0	6.0
C	1.1	10.5	9.6	34.0	16.0	1.0
B	1.0	10.1	9.8	29.0	9.0	6.0
D	0.9	8.0	8.7	13.0	4.0	1.4
E	0.9	6.8	7.3			
F	1.0	5.4	5.4		2.0	
Z	1.0	5.1	5.4			
Y	0.9	3.6	4.1			
X	1.0	2.7	2.7			
Total	1.3	261.7	199.2			
Overlap region	1.5	122.8	79.8	225.0	55.0	19.7

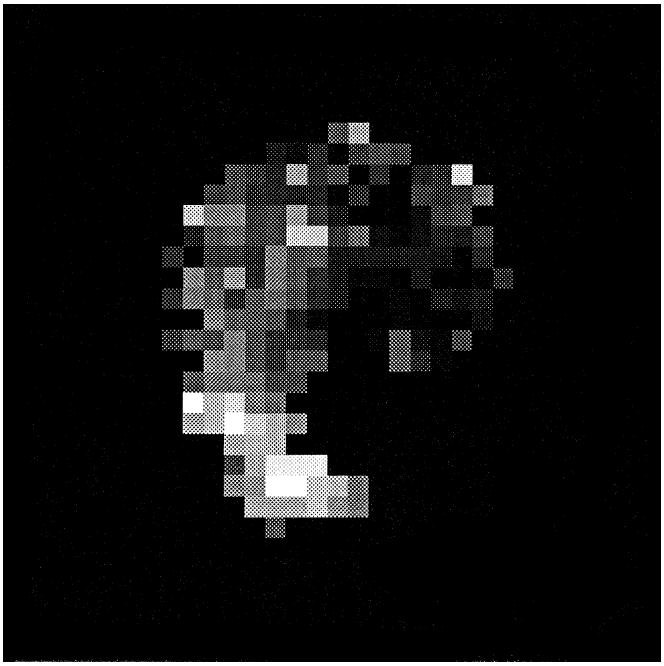

Fig. 3. Image of the ratio of [Ne III]/[Ne II] in the Antennae Galaxies. North is to the left. The highest ratio is the overlap region.

pseudo continuum is present between the 11.3 and the 12.7 μm emission bands creating the asymmetry observed in the [Ne II] line (Boulanger *et al.* 1996). The origin of this emission might be linked with duo and trio vibration modes of PAH molecules, but it remains to be confirmed. In the most active regions, the [Ne III] line at 15.5 μm is present above the thermal continuum due to hot dust. The imaging capability of the CVF offers a unique opportunity among the other ISO instruments to study the variation of spectral features from one area of the galaxy to the other.

The [Ne III] (15.5 μm) to [Ne II] (12.8 μm) ratio is very sensitive to the effective temperature of the ionizing stars (Rubin 1985). The line intensity of the [Ne II] line is uncertain due to blending with the 12.7 μm band which cannot be resolved due to the poor spectral resolution of the CAM CVF. However, we can determine an upper limit to the line intensity. We assume a continuum level as the mean value between the 11.3 and 12.8 μm emission features, and we computed line ratios using the peak intensities rather than the equivalent widths. The values derived in this way are consistent with the values derived from the high spectral resolution observation of the overlap region with the Short Wavelength Spectrometer (SWS) on board ISO, (Kunze *et al.* 1996). This demonstrates that our procedure is adequate, at least in the regions where the [Ne II] line dominates above the 12.7 μm band. Our estimation of the [Ne II] line is a upper limit of the true line intensity. The map of this ratio (figure 3) shows that there are large differences across the Antennae. The [Ne III] to [Ne II] ratio is 1 in the brightest area of the overlap region, and decreases to 0.1 or below in the central regions of NGC 4038 and in NGC 4039. Using the mean electron density n_e = 300 cm^{-3} derived from the ISO Long Wavelength Spectrometer (LWS) spectrum (Fischer *et al.* 1996) and SWS spectrum (Kunze *et al.* 1996), and H II region models computed for the Orion nebula abundances (Rubin 1985), we estimate a lower limit to the effective temperature of the ionizing stars to be 39,500 K in the overlap region and 37,000 K in the nuclei. Using the stellar evolutionary tracks of Maeder and Meynet (1987), and assuming an instantaneous starburst, this corresponds to ages of 2.5 and 3.5 10^7 years for the overlap and nuclei respectively. This general gradient of the [Ne III] to [Ne II] ratio can be interpreted in light of the dynamical interactions. The most active regions are where shocks, due to the two colliding gaseous disks, took place. Due to the galaxy rotation, this shocked region can move across the disk. With a disk rotation of 250 km s^{-1}, the motion can be as much as 3 kpc in 10^7 years, - the size of the most active region in the overlap area, assuming a distance of 20 Mpc. Another explanation would be an intrinsic difference in the IMF.

The 15 μm continuum intensity is well correlated with the [Ne II] and the [Ne III] line intensities. This confirms the

fact that this continuum is due to the thermal emission of hot dust heated by the absorption of the ionizing photons emitted by young stars. This is strengthened by the good correleation which exists between the 15 μm continuum map and the [Ne III]/[Ne II] ratio distribution, and the fact that the 15 μm intensity increases together with the [Ne III]/[Ne II] ratio. The [Ne III]/[Ne II] ratio is a measure of the hardness of the UV flux. This correlation indicates that the continuum intensity at 15 μm is very well correlated with the star formation activity. Since the LW3 filter is dominated by the thermal continuum beyond 13 μm and the two Ne emission lines, which are all correlated with the star formation activity, the LW3 intensity must be also a good indicator of the star formation. However a quantitative model which transforms the 15μm continuum, or the LW3 intensities, into a star formation rate is far from trivial. It depends on the characteristics of the UV flux, which are linked with the assumed IMF and age of the burst. Also necessary is knowledge of the composition of the dust grains and the details of the physical processes which control the photon absorption by the dust grains. Such a detailed model is needed since it is not possible to determine a bolometric correction for the grain emission. It would require far infrared measurements which cannot be obtained at the high spatial resolution as ISOCAM measures. Progress in this direction will require theoretical modeling, as well as observations of the Galactic HII regions to adjust the parameters of the model. This activity is in progress.

In contrast with the the correlations seen with the thermal continuum, there is an anticorrelation between the PAH-like emission features and the star burst activity. This is particularly striking in knot A which is almost devoid of 7.7 and 8.4 μm emission. A similar trend has already been observed in Galactic star formation regions (Verstrate *et al.* 1996). The PAH emission bands vanished in the center of HII regions. The anticorrelation is nevertheless not as clear as what is observed in the Galaxy, due to the poor resolution of ISOCAM. A single resolution element, at the distance of the Antennae system (5" $\simeq 500pc$) encompasses the central HII region and the associated PDR where PAH emissions are predominant.

5. Conclusions

From the ISOCAM 6.7 and 15 μm images of the Antennae Galaxies, we find that the region of overlap due to the colliding galaxies, contributes approximately half of the total luminosity of the entire system. The CVF spectra of the whole system show that the 15 μm is due to thermal emission from hot dust heated by young stars. The overlap region is the most active star forming region of the system. From the [Ne III]/[Ne II] ratio we find a lower limit to the effective temperature of the ionizing stars of 39,500 K in the overlap region and 37,000 K in the nuclei.

References

Boulanger, F. *et al.* 1996, A&A this volume
Césarsky, C. *et al.* 1996, A&A this volume
Fischer, J. *et al.* 1996, A&A this volume
Hummel, E. and van der Hulst, J. M. 1986, A&A 155, 151
Kessler, M.F. *et al.* 1996, A&A this volume
Keel, W.C., Kennicutt, R. C., Hummel, E. and van der Hulst, J. M. 1985, A.J. 90, 708.
Kunze, D. *et al.* 1996, A&A this volume
Maeder, A. & Meynet, G. 1987, A&A 182, 243
Rubin, R. 1985, ApJ Supp 57, 349
Sanders, D. B., Soifer, B. T., Elias, J. H., Madore, B. F., Matthews, K., Neugebauer, G. and Scoville, N. Z. 1988, ApJ 325, 74
Sanders, D.B. & Mirabel, I.F. 1985, ApJ 298, L31
Sauvage, M. *et al.* 1996, this volume
Soifer, B. T., Sanders, D. B., Neugebauer, G., Danielson, G. E., Lonsdale, C. J., Madore, B. F. and Persson, S. E. 1986, ApJ(Letters) 303, L41.
Stanford, S.A., Sargent, A.I., Sanders, D.B. & Scoville, N.Z. 1990, ApJ 349, 492
Starck, J.-L., Claret, A. and Siebenmorgan, R., C.E.A. Technical Report, March, 1996
Verstraete *et al.* 1996, A&A this volume